PART 7

INFRARED TECHNOLOGY AND THE FUTURE

https://doi.org/10.1017/S0074180900124854 Published online by Cambridge University Press

PROSPECTS IN ADAPTIVE OPTICS FOR SOLAR APPLICATIONS

FRANÇOIS RODDIER AND J. ELON GRAVES
Institute for Astronomy, University of Hawaii at Manoa, 2680 Woodlawn Drive, Honolulu, HI 96822, U.S.A.

Abstract. We review the theoretical perspective for problems in adaptive optics, outline recent progress, and consider its application in the infrared. Techniques in adaptive optics are on the threshold of revolutionizing modern astronomy. These techniques are particularly applicable in the infrared, where refractive effects of turbulence are reduced, characteristic cell sizes are greater, and the isoplanatic patch diameter is increased. Adaptive techniques could be especially appropriate for modern large solar telescopes now under consideration that could operate in the infrared.

Key words: atmospheric effects – Sun: general – techniques: miscellaneous – telescopes

1. Introduction

The terms "active optics" and "adaptive optics" are commonly used. Active optics can be regarded as adjustments in telescope optics designed to correct for telescope induced aberrations, such as misalignment and mirror deformation. Adaptive optics refers to active optics to correct for atmospherically induced aberrations, *i.e.*, seeing. The basic operation of adaptive optics is illustrated conceptually in Figure 1. Light from the imaging system, which includes an adaptive optical corrector is imaged onto a wavefront sensor and a camera. The wavefront sensor assesses the aberrations and this information is converted by control electronics to electrical signals that drive the corrector. The camera simply records the corrected image.

2. Theoretical Review

In practice, it is only possible to correct the actual aberration approximately. The corrector is only capable of a finite number, N, of degrees of freedom. The wavefront perturbations the corrector can produce may be represented as a linear combination of modes that span a manifold of dimension N. These modes are most conveniently chosen to be functions of location in the system pupil, which can be chosen so as to be orthogonal under an appropriate inner product. Several systems of modes are used. For theoretical calculations one uses:

1. *The Karhunen-Loeve Modes*: the set of orthogonal functions which best matches the statistics of atmospheric turbulence – *i.e.*, the statistically-independent modes. For an adaptive optics system with N degrees of freedom the best possible compensation is achieved by compensating the first N Karhunen-Loeve modes.

2. *The Zernike Modes*: commonly used in optics because of their simple analytic expression.

The actual modes that characterize a certain physical system with are called the *system modes.*

D. M. Rabin et al. (eds.), Infrared Solar Physics, 557–566.

https://doi.org/10.1017/S0074180900124854 Published online by Cambridge University Press

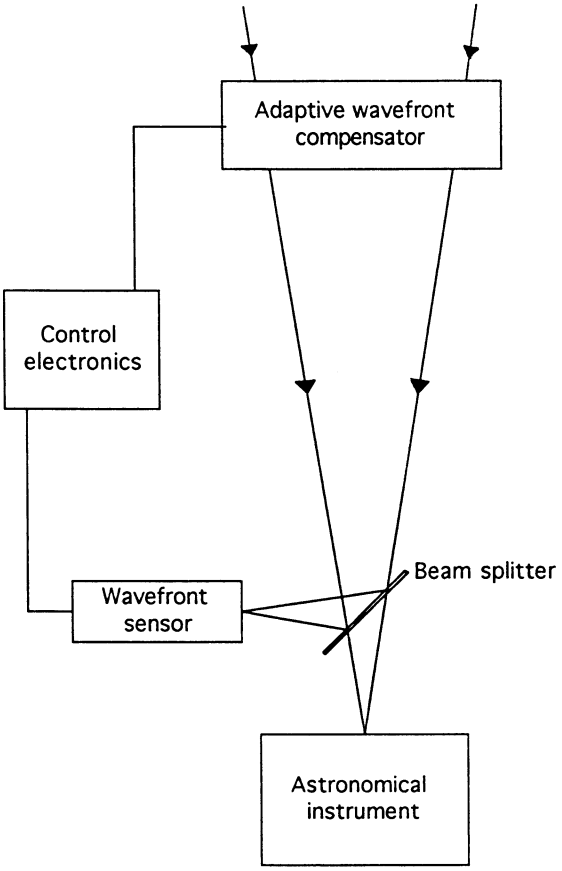

Fig. 1. Schematic of the general active- or adaptive-optical system.

Details regarding the Zernike modes are discussed by Born and Wolf (1975). Similar to cylindrical harmonics, they are represented by functions of the following form:

$$Z_{nm}(\rho,\theta) = P_{nm}(\rho)e^{im\theta}, \tag{1}$$

where the radial functions, P_{nm}, are polynomials of finite degree, n. These "Zernike polynomials" share the property of Bessel functions that only terms of order $|m|+2l$ are included, where l must be an integer greater than or equal to zero. Thus, the limiting degree, n, must satisfy $n \geq |m|$, and $n - |m|$ is even. Table I lists how the lowest-order aberrations are characterized in terms of the Zernike modes.

Parameters customarily used for expressing the performance of an optical system are largely based on the "Strehl intensity", I_0, the central intensity in the degraded point-source image. The "Strehl ratio" is defined by $R \equiv I_0/I_{\max}$, the ratio of the Strehl intensity, I_0, to the central intensity in the diffraction-limited

https://doi.org/10.1017/S0074180900124854 Published online by Cambridge University Press

TABLE I
The Zernike Aberrations

$n \setminus m$	0	1	2	3	4	5
0	piston					
1		tip-tilt				
2	defocus		astigmatism			
3		coma		(coma)		
4	spherical		(astigmatism)			

image. The "normalized Strehl ratio", $R/R_{\max}$, is the Strehl ratio, R, of a particular adaptive-optics system being considered normalized by the Strehl ratio, $R_{\max}$, of an uncompensated image observed through an infinitely large telescope. This normalized Strehl ratio, $R/R_{\max}$, normally depends only on the ratio, D/r_0, of the telescope diameter, D, to Fried's seeing parameter, r_0. For the exact definition of r_0, we refer to Fried (1966); however r_0 can be roughly regarded as the separation in the entrance pupil over which the rms wavefront error approaches one wavelength, λ.

The theory implies that the statistics of atmospheric turbulence can be properly characterized as a function of scale size. A formalism for this was developed by Fried (1966), based on turbulence described by a "wave structure function" that expresses the correlation in wave perturbations over a separation r in the entrance pupil. Fried characterizes the wave structure function as proportional to $r^{5/3}$ based on the Kolmogoroff rule on the statistics of atmospheric turbulence. We note that r_0 is strongly dependent on wavelength, λ, since the scale over which a wavefront perturbation approaches a greater wavelength must be greater, according to the $r^{5/3}$ rule. It is then possible to express the Strehl ratio for a particular system for correcting wave-fronts as a function of the ratio D/r_0 alone.

Figure 2 shows computations of the dependence of the normalized Strehl ratio, $R/R_{\max}$, on D/r_0, made by N. Roddier (1990) for Zernike corrections of various orders. Note the strong dependence of D/r_0 on λ, by comparing the upper and lower abscissa scales. The upper scale approximately applies to the McMath telescope under average seeing conditions. The normalized Strehl ratios for various Zernike orders of correction all rise initially in proportion to D/r_0, but eventually fall away from the diffraction limit, culminating at a critical D/r_0 and thence dropping rapidly toward the envelope for uncorrected optics. This behavior is summarized as follows:

1. A given adaptive-optics system provides a maximum image improvement at a critical ratio, $(D/r_0)_c$, at which the trade-off between diffraction-limited optics and seeing conditions is optimized.
2. At this optimum trade-off the Strehl ratio, R (un-normalized) is 0.3.
3. The number of degrees of freedom of the system can be much smaller than $(D/r_0)_c^2$ (typically 7 times smaller).

https://doi.org/10.1017/S0074180900124854 Published online by Cambridge University Press

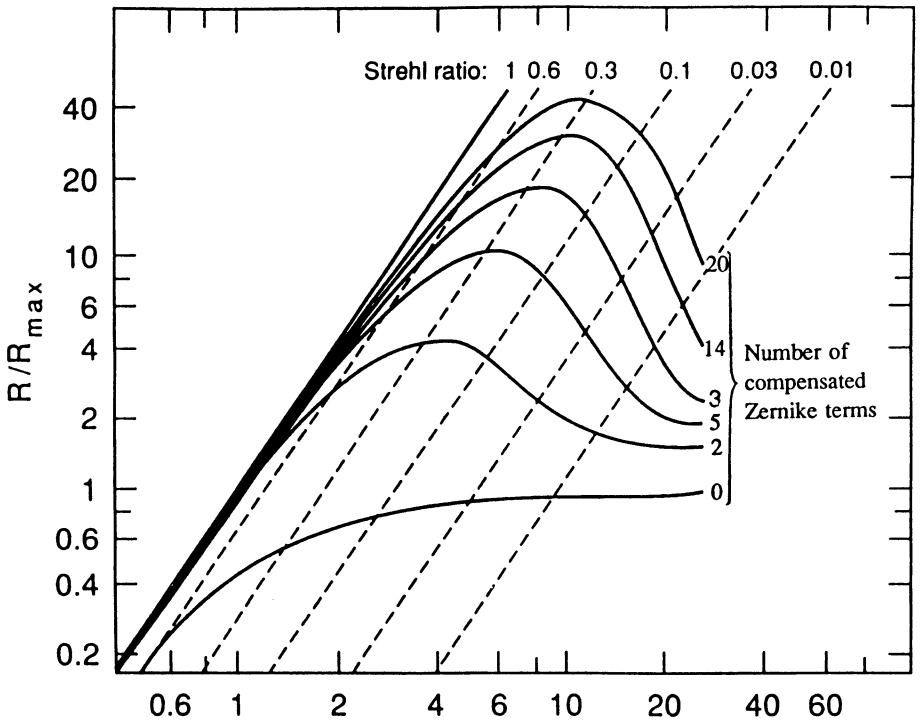

Fig. 2. Improvement in the Strehl Ratio (R/R_{max}) for various orders of Zernike correction.

4. A Strehl ratio higher than 0.3 can be obtained only at a high cost. As a consequence, the system bandwidth and the reference source brightness required also increase, while the isoplanatic patch size decreases.

5. In most cases, a Strehl ratio higher than 0.3 is not necessary to obtain diffraction-limited images. Images and data from imaging spectrographs can be easily deconvolved when a Strehl ratio of 0.3 is reached.

For moderate values of D/r_0, *i.e.*, relatively small telescopes or good seeing conditions, corrections encompassing only a few degrees of freedom, perhaps only tip-tilt, can drastically improve image quality. Simple tip-tilt correction (2 degrees of freedom) is now a well-practiced art, particularly with relatively small telescopes, for which image motion alone may prevent attainment of the diffraction limit in extended exposures. For larger telescopes, requiring more degrees of correction, 5 to 10 degrees of freedom are now being tested with great success (Roddier 1991). While it is useful to further increase the flexibility of the correction as D/r_0 increases, and more sophisticated correctors can be expected in the future, the required degrees of freedom needed, eventually become oppressive for large D/r_0. The infrared, then offers a powerful handle for keeping D/r_0 within practical limits for larger apertures.

https://doi.org/10.1017/S0074180900124854 Published online by Cambridge University Press

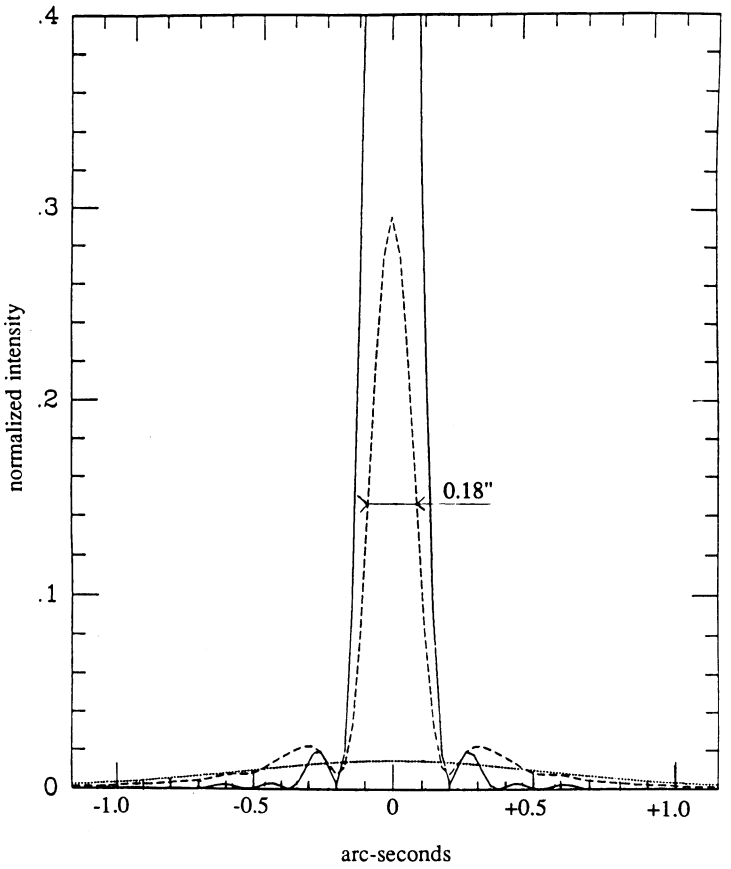

Fig. 3. Point source response functions for a 1.5 m telescope in 1.2 μm radiation for (dotted curve) uncompensated seeing that is 1.5″ in visible light and for (dashed curve) a 9-order Zernike correction. The solid curve shows the diffraction limited response of the telescope free from seeing aberrations.

3. An Example: Point Source Profiles

Figure 3 shows how the time-averaged point source profile looks for the 9-mode Zernike correction at its optimum D/r_0, for a Strehl ratio of 0.3. This simulation is made for a 1.5-m telescope at 1.2 μm in conditions under which the seeing in visible light is 1.5″. The dotted curve shows the point-source response of the telescope uncorrected for seeing aberrations. The dashed curve shows the profile with the 9-mode Zernike correction. The result is a substantial diffraction-limited core containing the expected 0.3-fraction of the core power of a perfect, diffraction-limited system (solid curve). Such a system would allow full diffraction-limited (0.18″) reconstruction of an image with only moderate losses in signal to noise. The foregoing

https://doi.org/10.1017/S0074180900124854 Published online by Cambridge University Press

TABLE II
Projected Characteristics for an Adaptive Optics System for the McMath Telescope

λ	D/r_0	N	θ	B
0.5 μm	25	90	2.6″	250 Hz
0.8 μm	14	28	7″	125 Hz
1.2 μm	8.7	11	15″	75 Hz
1.6 μm	6.2	5	30″	50 Hz
2.2 μm	4.2	2	60″	30 Hz

theoretical considerations can be summarized by the following 5 points, which are discussed in greater detail by Roddier, Northcott, and Graves (1991). Further theoretical modeling in terms of residual wave-front errors is described by Chassat (1989).

The ratio D/r_0 serves as a useful guideline for anticipating system requirements for a particular telescope under typical seeing conditions as well as performance qualities that can be anticipated. System requirements include the number of degrees of freedom, N, and the electronic loop bandwidth, B, needed to process the correction. Performance qualities include the angular diameter, θ, of the compensated field of view (the isoplanatic patch). Table II summarizes these parameters for conditions typical at the McMath Telescope in terms of operation at the optimum Strehl ratio, $R = 0.3$, over a range of wavelength. System requirements are greatly relaxed in the infrared, while performance is greatly enhanced.

4. Practical Realization

The technical tasks confronting adaptive optics can be separated into two main categories: (1) wavefront sensing and (2) wavefront correction. Several schemes for wavefront sensing are under development, some having already attained considerable success, particularly in the case of stellar applications with objects that have sufficiently bright and sharp stellar references (see Fig. 4). Among these are the following:

The Shack-Hartmann Sensor: This device (Fig. 4*a*) analyzes the image displacement in individual subregions of the pupil, which is related to the wavefront slope in each subregion.

The Itek sensor: A Ronchi ruling moves across the image plane producing a modulation in the pupil image (Fig. 4*b*). The phase of the modulation at a given pupil point depends on where the corresponding rays are intercepted and gives a measure of the slope of the local wavefront.

The Curvature Sensor: This scheme (Fig. 4*c*) works by differencing pupil intensity maps measured in front of and behind the focus. The normalized difference,

$$S = \frac{I_1 - I_2}{I_1 + I_2},$$

https://doi.org/10.1017/S0074180900124854 Published online by Cambridge University Press

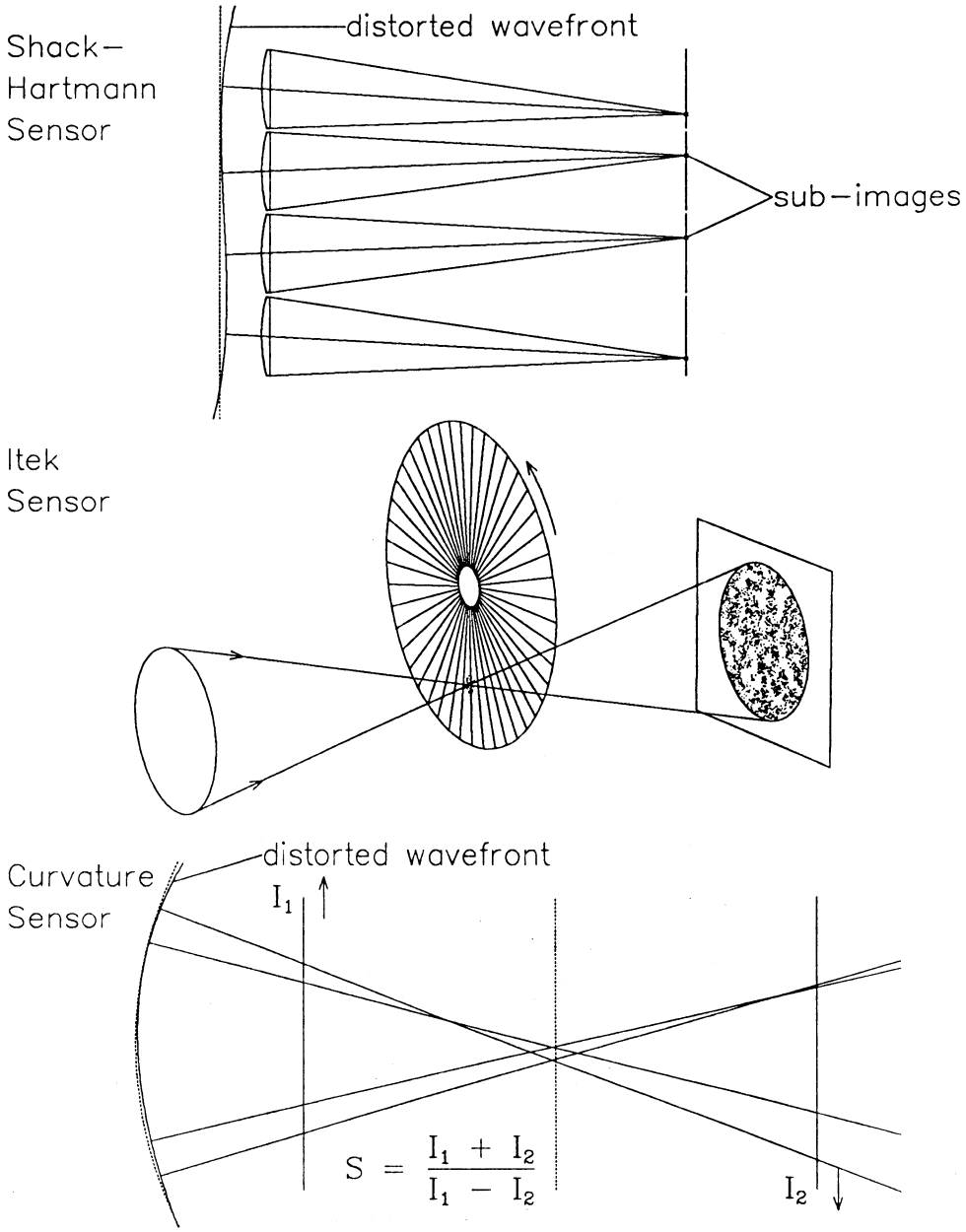

Fig. 4. Wavefront sensors for stellar applications.

https://doi.org/10.1017/S0074180900124854 Published online by Cambridge University Press

gives a good approximation of curvature. This can be seen by considering that a positive perturbation in wavefront curvature draws the focus toward the near-side plane, resulting in a local enhancement of the intensity, I_1, in the pupil in this plane as compared with an intensity dilution of the intensity I_2, in the far-side plane. A negative perturbation in curvature acts *vice versa*.

Sensors built for stellar applications will also work for solar applications (although less efficiently) using a dark spot as a reference. This has already been demonstrated with both the ITEK and Shack-Hartmann sensors, and there is no doubt that similar performance can be obtained with a curvature sensor. Special wavefront sensors can be built for solar applications that work on extended sources, such as the solar granulation. Instead of measuring intensities, one has to measure the variance or covariance of intensity fluctuations. Current schemes under development include

- an array of correlation trackers (Sacramento Peak) (complex and expensive), and
- image sharpening with a dither mirror (LEST) (expensive and probably too slow).

The concept of curvature sensing could also be extended to variance measurements and provide a way to build a *simple* and *less expensive* high-speed solar wavefront sensor. This could be based simply on difference measurements in granular contrast on either side of the focal plane for the image formed by a particular region of the pupil analyzed to determine defocus due to wavefront curvature.

We have made considerable recent progress in wavefront correction. The scheme we have developed at the University of Hawaii is based on curvature sensing and compensation. The wavefront correction is based on a deformable piezo-bimorph mirror, made in collaboration with the Office National d'Etudes et de Recherches Aerospatiale in France. This is a thin double wafer of two materials of the same piezo-electric polarity, so that electric fields applied in opposite directions induce a differential warping of the two components, which results directly in an induced curvature. In our present application, the wafer, 6 cm in diameter, is partitioned into 13 electrically separate regions, as shown in Figure 5. The outer surfaces are uniformly covered with a thin conducting film that acts as a common ground electrode. The inner surface is also covered with a thin conducting layer, but partitioned into separate electrodes, each connected to its respective driver. In our application, the actual pupil occupies only the inner 7 regions. However, the outer regions of the membrane are needed for the function of setting appropriate outer boundary conditions. Figure 6 shows comparative time averaged-profiles obtained by this system in the laboratory.

5. Summary

Image enhancement based on wavefront sensing and correction by active optics is now making the transition from a very promising prospect to a broad range of immediate, practical scientific applications. This will probably revolutionize stellar astronomy. There is every reason to anticipate that the techniques now being

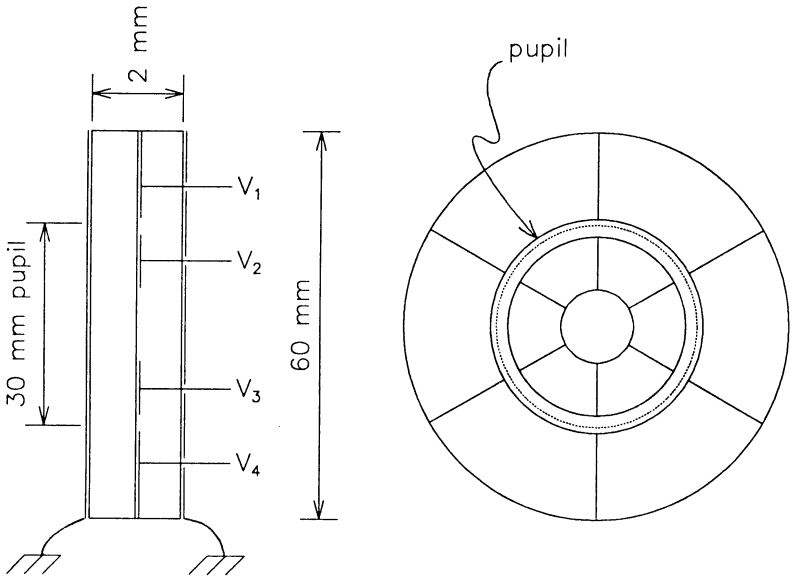

Fig. 5. The University of Hawaii deformable piezo-bimorph mirror.

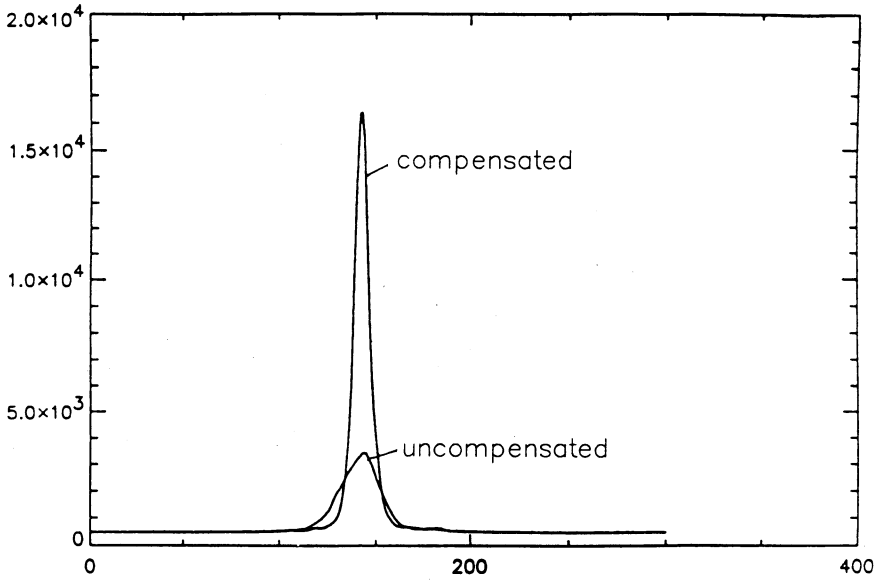

Fig. 6. Comparative time-averaged intensity profile of seeing-uncompensated and compensated point source images.

https://doi.org/10.1017/S0074180900124854 Published online by Cambridge University Press

successfully applied in stellar observations can be extended to solar applications. Moreover, active optical techniques are *particularly* well suited to the infrared.

References

Born, M. and Wolf, E.: 1975, *Principles of Optics*, Pergamon Press, New York, p. 464.
Chassat, F.: 1989, *J. Opt.* (Paris) **20**, 13.
Fried, D. L.: 1966, *J. Opt. Soc. Am.* **56**, 1372.
Roddier, F., Northcott, M., and Graves, J. E.: 1991, *Pub. Astron. Soc. Pac.* **103**, 131.
Roddier, N.: 1990, *SPIE Conf. Proc.* **1237**, 668.